JOURNAL OF MECHANICAL ENGINEERING AND SCIENCES
ISSN: 2289-4659 e-ISSN: 2231-8380
VOLUME 20, ISSUE 2, 2026, 11149 - 11163
DOI: https://doi.org/10.15282/jmes.20.2.2026.2.0870

RESEARCH ARTICLE

Shear-wave modulation in a dry sandy–Piezoelectric–fibre-reinforced trilayer model: A closed-form electro-mechanical approach under smooth contact

Suparna Roychowdhury[1], Mostaid Ahmed[2]*, Ayan Chatterjee[3], Abhijit Pramanik[4]

[1]Department of Mathematics, Brainware University, Barasat, West Bengal, 700125, India
[2]Mathematics Division, School of Advanced Sciences and Languages (SASL), VIT Bhopal University, Kothrikalan, Sehore, Madhya Pradesh-466114, India
[3]School of Science and Technology, The Neotia University, Sarisha, West Bengal 743368, India
[4]Department of Basic Science, MCKV Institute of Engineering, Howrah, West Bengal, 711204, India

Abstract – The article exquisitely delves to study the transmission of shear waves (SH) in a tri-layered geological media which is fundamental to nondestructive testing and SAW devices, including a piezoelectric layer sandwiched between a dry sandy half-space and a fiber-reinforced half-space under smooth-contact conditions. The analyticall study investigates the transference of SH waves through such a configuration, aiming to derive the complex dispersion relation and asses the inpact of sandy parameters, fiber reinforcement anisotropy, piezoelectric coupling and thickness of layer on phase velocity and mode confinement. Using the Biot's theory for dry sandy media, constitutive relations for fiber-reinforced elastic materials and linear piezoelectricity under quasi-static approximation, the governing equations are formulated and solved via potential functions under smooth contact boundary conditions, stress and displacement continuity, vanishing stress at the upper interface and open-circuit electrical conditions producing the secular equation, which is then evaluated numerically. Results demonstrate that the phase velocity remains heavily sensitive to the reinforcement anisotropy and the frictional coefficient of the dry sandy medium; the piezoelectric layer introduces electromechanical coupling that generates distinct dispersion branches and band gaps at high wavenumbers, while smooth contact effectively confines energy within the layered structure. The model offers immediate applications in smart seismic wave barriers, improved inversion of shear-wave splitting in desert regions underlain by reinforced strata, and piezoelectric surface acoustic wave sensors for structural health monitoring. By bridging classical geomechanics and modern smart materials, this model may serve as a rigorous benchmark for future experimental and computational studies.

Article History
Received : 25 May 2025
Revised : 7 April 2026
Accepted : 15 June 2026
Published : 30 June 2026

Keywords
SH-waves
Dry sandy layer
Piezoelectricity
Fiber reinforced layer
Disperson relation

1. Introduction

A field of study called theoretical seismology examines how waves propagate through the Earth's stratified structure. Similar to the layers of an onion, the interior of the Earth is commonly described as a sequence of concentric spherical layers, each having distinct thicknesses and mechanical properties. These layers include the outer and inner cores, crust, and mantle. Each of these layers has unique compositions, temperatures, and physical states.Crust fractures and deformations of the earth as a result of stresses brought on by subterranean explosions (e.g., nuclear testing), fault ruptures, and other geological activity. Large volumes of energy are released by these events, and these waves of energy move through Earth in an elastic manner. These waves undergo changes in direction and speed as they pass through various materials, depending on the characteristics of each layer and provide crucial information on the interior structure of Earth as they move from their source to the surface. Scientists can ascertain the configuration and disposition of the distinct rock layers by examining these waves. Understanding the Earth's geological structure and locating important resources such as water, minerals, metals, hydrocar bons, and petroleum depends on this knowledge.The surface of the Earth is traversed by a specific type of wave known as a surface wave. Because surface waves can significantly shake the ground, they are particularly important in seismology for understanding earthquakes and other seismic events. The study of elastic wave propagation through the layered medium of Earth is still highly useful for understanding natural dangers and exploring new resources.Seminal works on surface wave propagation include publications by authors such as Achenbach [1]. Li [2] used com plex propagation functions to investigate the dispersive nature of SH-waves in a homogeneous three-layered model and elastic two-layered half-space. It is possible to describe the soil layer as sand-like rather than elastic. Sand particles in a dry sandy mantle do not hold moisture or vapor from the atmosphere. As seismologists are getting much more cuious on propagation of elastic waves in dry sandy media because of their many utilitarian aspects. The mechanics of dry sandy soil were investigated by Weiskopf [3], who also offered pertinent connections for this type of medium. The propagation of seismic waves can be affected by a variety of interfacial characteristics,such as flaws and irregularities, therefore it is imperative to understand wave propagation in elastic media, especially when taking different boundary conditions into account. A detailed analysis was carried out by Paul [4] on transference of Love waves in a dry sandy layer intertwined among two substrates. Numerous schol ars, including Slavin and Wolf [5], Wolf [6], and Chattopadhyay and Pal [7], have looked into the effects of abnormalities. Shear waves in viscoelastic medium with various forms of irregularities was demonstrated by Chattopadhyay [8]. Furthermore, the effects of starting stress and gravity on torsional surface waves in a dry sandy medium were investigated by Dey et al. [9].Singh [10] investigated the Love

*CORRESPONDING AUTHOR | **Mostaid Ahmed** | ✉ mostaidahmed@yahoo.in

wave's propagation in an corrugated layered material contains irregularity. Initially strained sandy layer overlying an anisotropic porous substrate was discussed by Pal and Ghorai [11] by taken into account the effects of gravity. The dispersion relation for this model was derived by Pandit and Kundu [12] through an examination of Love wave prop agation in a viscoelastic sandy layer over an initially stressed orthotropic semi-infinite substrate. Love wave propagation in a dry, sandy medium over an isotropic half-space with an imperfect interface was studied by Deep and Verma [13], who revealed the effects of the degree of imperfection and the sandiness parameter. It is commonly known fact that sensors and transducers use Love waves that propa gate through piezoelectric materials. Layered models involving inhomogeneous boundary conditions, like thin films, are often used to improve the performance of these devices. Because Love waves have wider applications, a lot of research has been done to examine their properties in multilayer piezoelectric systems. The propagation of Love waves in multilayer piezoelectric devices has been the subject of extensive published re search. Acoustic wave energy in a guiding layer put on top of a piezoelectric surface was covered by Liu et al. [14]. According to Han et al.[15] , and graded functional materials have an impact on these systems. Furthermore, Du et al. [16] looked into the effect of starting stress on Love wave propagation in such layered structures, while Eskandari et al. [17] researched dissipation in piezoelectric layered structures for Love wave propagation. Different types of hard or soft rocks or materials with self-reinforcing qualities may be found in the Earth's crust. Fiber-reinforced materials can be made of metal whiskers, carbon, or nylon. Seismic wave propagation through reinforced medium is important for applications in soil mechanics, architecture, mining, civil engineering, and geophysical prospecting. In their study of plane wave propagation in fiber-reinforced elastic media, Singh and Singh [18] showed that the angle formed by the propagation direction and the reinforcement direction determines the phase velocities of quasi P- and SV-waves. They also demonstrated on how these elastic waves would bounce off the free surface of an elastic half-space reinforced with fibers. Because Love waves have significant uses, researchers from a variety of fields have conducted numerous investigations to analyse their characteristics in multilayer piezoelectric structures [19–34]. Recently Hafizi et al. [35] demonstrated how the wave scattering impacts due to defects in damaged areas in thin laminated composite plates. Fajril et al. [36] and Majid et al. [37] vividly characterized how the waves behave under stress-strain relations and flexural configuration with fiber-reinforced composites. In this paper, we have considered a three-layered model for Love wave propagation. Since Earth is considered as multi-layer model so here we try to investigate properties of Love wave propagation fits into multi-layer model or not. Along with Piezoelectric layer and Fiber reinforced layer, we have incorporated here another layer in that problem and that is Dry sandy layer which we have been used here. The interplay between these layers highlights the importance of considering multi-material interactions in wave propagation studies. The piezoelectric layer, in particular, offers promising avenues for advanced technological applications.

2. Materials and Methods

2.1 Problem Formulation

To study the propagation of SH- waves, we consider a model featuring a piezoelectric layer situated between two half-spaces. The upper half-space consists of dry sandy, while the lower half-space is fiber-reinforced. Both the fiber-reinforced and the piezoelectric layer are presumably having some initial stresses due to loads, thereby altering the mechanical state prior to any wave transmission. A three-dimensional Cartesian framework (x, y, z) is adopted to formally describe the problem (Fig 1). The origin is positioned at the common interface separating the piezoelectric layer from the lower half-space, and the positive z-axis is directed vertically downwards. Thereby making the domain (-H<z<0) to correspond the piezoelectric region, the interval (z<-H) to represent the dry sandy half-space and the region (z>0) to characterize the fiber-reinforced medium. Wave motion is presumed to occur along the x-direction. Under the assumption of horizontally polarized SH-wave propagation, the displacement components satisfy (u=w=0), while the sole non-vanishing displacement component is expressed as (v=v(x,z,t)). Here, v_i (i = 1,2,3) denotes the displacement field associated with the individual media. The subscripts (1), (2), and (3) are employed to distinguish parameters for the dry sandy half-space, the piezoelectric layer, and the fiber-reinforced semi-medium respectively. Figure 1 shows the schematic diagram of the problem.

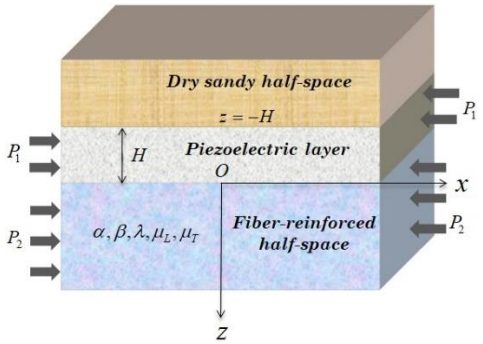

Figure 1. Schematic diagram of the problem

2.2 Dynamical Equation and Solution of Dry Sandy Half Space

The equation of motion for the propagation of SH- wave, assuming that there is no body force present, is written as (Kar et al. [38])

$$\tau^1_{ij,j} = \rho_1 \frac{\partial^2 v_i}{\partial t^2} \tag{1}$$

The stress-strain relation corresponds to dry sandy medium can be written as

$$\tau^1_{ij,j} = \lambda\theta\delta_{ij} + 2\frac{\mu_1}{\eta_1}e_{ij} \tag{2}$$

where the respective variables λ and μ_1 are the Lame's constants, ρ_1 uses for the identification of density of the material, η_1 notation can be taken for sandiness parameter, δ_{ij} signifies as Kronecker's delta, τ^1_{ij} designates for the components of stress and e_{ij} symbolizes strain tensor and $\theta = e_{11} + e_{22} + e_{33}$ indicates the strain in volume.

Thus, with the help of description given above for SH- type wave propagation, the components for stress are

$$\tau^1_{11} = \tau^1_{22} = \tau^1_{33} = \tau^1_{13} = 0$$

$$\tau^1_{12} = \tau^1_{21} = \frac{\mu_1}{\eta_1}\frac{\partial v_1}{\partial x}$$

$$\tau^1_{23} = \tau^1_{32} = \frac{\mu_1}{\eta_1}\frac{\partial v_1}{\partial z}$$

Therefore, the governing equation of motion from Eq. (1) becomes,

$$\frac{\mu_1}{\eta_1}\left[\frac{\partial^2 v_1}{\partial x^2} + \frac{\partial^2 v_1}{\partial z^2}\right] = \rho_1 \frac{\partial^2 v_1}{\partial t^2} \tag{3}$$

where μ_1, η_1 and ρ_1 are rigidity, density and sandiness parameter, respectively.

Let us consider the solution of Eq. (3) is

$$v = V_1(z) \tag{4}$$

Then Eq. (3) reduces to,

$$\frac{d^2 V_1}{dz^2} - \varsigma_1^2 V_1 = 0 \tag{5}$$

where $\varsigma_1^2 = k^2\left(1 - \frac{c^2}{c_1^2}\right)$ and $c_1^2 = \frac{\mu_1}{\eta_1\rho_1}$

Therefore, the solution of Eq. (5) can be written as,

$$V_1 = A_1 e^{s_1 z} + B_1 e^{-s_1 z}$$

where A_1 and B_1 are the respective arbitrary constants.

As $z \longrightarrow -\infty$, there is no displacement in the upper half-space, i.e., $\lim_{x\to-\infty} v_1 = 0$,

So, $\lim_{x\to-\infty} V_1 = 0$

For propagation of SH- waves the term s_1 must be positive and real.

So, for the dry sandy upper half space

$$v_1 = A_1 e^{s_1 z} e^{ik(x-ct)} \tag{6}$$

2.3 Solution of Piezoelectric Layer

The Equation of motion for SH- waves with respect to the mechanical-electrical coupled PDE and electrical PDE related to displacement, may be presented as, (Gupta et al. [29])

$$c_{44}\Delta^2 v_2 + e_{15}\Delta^2\phi - \frac{P_1}{2}\frac{\partial^2 v_2}{\partial x^2} = \rho_2 \frac{\partial^2 v_2}{\partial t^2}$$
$$e_{15}\Delta^2 v_2 = \varepsilon_{11}\nabla^2\phi \tag{7}$$

where Δ^2 refers to the Laplace operator of two-dimensional and ρ_0 refers to the density of the middle layer i.e., piezoelectric layer.

$$\sigma^2_{yz} = c_{44}\frac{\partial v_2}{\partial z} + e_{15}\frac{\partial\phi}{\partial z}$$
$$\sigma^2_{xy} = c_{44}\frac{\partial v_2}{\partial x} + e_{15}\frac{\partial\phi}{\partial x} \tag{8}$$

$$D_z = e_{15}\frac{\partial v_2}{\partial z} - \varepsilon_{11}\frac{\partial\phi}{\partial z}$$
$$D_x = e_{15}\frac{\partial v_2}{\partial x} - \varepsilon_{11}\frac{\partial\phi}{\partial x} \tag{9}$$

The substitution, we use

$$\psi = \phi - \frac{e_{15}}{\varepsilon_{11}} \tag{10}$$

reduces Eq. (7) into

$$c_{44}^{*} \nabla^2 v_2 - \frac{P_1}{2}\frac{\partial^2 v_2}{\partial x^2} = \rho_2 \frac{\partial^2 v_2}{\partial t^2}$$
$$e_{15} \nabla^2 \psi = 0 \tag{11}$$

where $c_{44}^{*} = c_{44} + \frac{e_{15}^2}{\varepsilon_{11}}$

Let us assume the following solution for Eq. (11)

$$v_2 = V_2(z)e^{ik(x-ct)}$$
$$\psi = \psi(z)e^{ik(x-ct)} \tag{12}$$

where the constants k, c represents the respective wave number and the phase velocity, also $v_2(z)$, $\psi(z)$ constitutes the respective solutions of

$$\frac{d^2V_2}{dz^2} + k^2 b_1^2 V_2(z) = 0$$
$$\frac{d^2\psi}{dz^2} - k^2\psi(z) = 0 \tag{13}$$

where, $b_1^2 = \left(\frac{c^2}{c_0^2} + \frac{P_1}{2c_{44}^{*}} - 1\right)$ and $c_0 = \sqrt{\frac{c_{44}^{*}}{\rho_2}}$

Therefore, the two solutions for Eq. (13) are

$$V_2(z) = C_1\cos(kb_1 z) + C_2\sin(kb_1 z)$$
$$\psi(z) = C_3 e^{kz} + C_4 e^{-kz} \tag{14}$$

where the mentioned C_1, C_2, C_3, C_4 demonstrate constants.
So, the final solution of the displacement components and the electric potential can be expressed as:

$$v_2(x,z,t) = (C_1\cos(kb_1 z) + C_2\sin(kb_1 z))e^{ik(x-ct)}$$
$$\phi(x,z,t) = \left[\frac{e_{15}}{\varepsilon_{11}}(C_1\cos(kb_1 z) + C_2\sin(kb_1 z)) + C_3\exp(kz) + C_4\exp(-kz)\right]e^{ik(x-ct)} \tag{15}$$

2.4 Dynamics and Solution of Fiber-Reinforced Half Space with Initial Stress

The primary Equation for an anisotropic, linearly elastic fibre-reinforced medium was proposed by (Belfield et al. [39])

$$\tau_{ij}^{3} = \lambda e_{kk}\delta_{ij} + 2\mu_T e_{kk} + \alpha\left(a_k a_m e_{km}\delta_{ij}\right) + 2(\mu_L - \mu T)\left(a_k a i e_{kj} + a_k a_j e_{ki}\right)$$
$$+\beta\left(a_k a_m e_{km} a_i a_j\right)\ , i,j,k,m = 1,2,3 \tag{16}$$

where τ_{ij}^{3} are stress components, $e_{ij} = \frac{1}{2}\left(\frac{\partial v_i}{\partial x_j} + \frac{\partial v_j}{\partial x_i}\right)$ are the strain components, δ_{ij} indicates the Kronecker delta. $\vec{a} = (a_1, a_2, a_3)$refers to preferred direction of reinforcement so that $a_1^2 + a_2^2 + a_3^2 = 1$. The vector $\vec{a}$ is the unit vector in fiber direction with the indices supposed to take values 1,2,3. Here β and $(\mu_L - \mu_T)$ denotes parameters of reinforcement and α represents material anisotropy coefficient. μ_T supposed to take for the shear modulus in transverse to the fibers, μ_L identifies for shear modulus along the fibers. Here λ is used for denoting Lame's constant.

So, the basic equation for how SH-waves move can be written like this:

$$\frac{\partial\tau_{21}^{3}}{\partial x} + \frac{\partial\tau_{23}^{3}}{\partial z} - \frac{P_2}{2}\frac{\partial\omega_{21}}{\partial x} = \rho_3\frac{\partial^2 v_3}{\partial t^2} \tag{17}$$

where,

$$\tau_{12}^{3} = \tau_{21}^{3} = \left[\mu_T\frac{\partial v_3}{\partial_x} + (\mu_L - \mu_T)\left(a_1^2\frac{\partial v_3}{\partial x} + a_1 a_3\frac{\partial v_3}{\partial z}\right)\right]$$
$$\tau_{23}^{3} = \tau_{32}^{3} = \left[\mu_T\frac{\partial v_3}{\partial_z} + (\mu_L - \mu_T)\left(a_1 a_3\frac{\partial v_3}{\partial x} + a_3^2\frac{\partial v_3}{\partial z}\right)\right]$$

and

$\omega_{21} = \frac{1}{2}\left(\frac{\partial v_2}{\partial x} - \frac{\partial v_1}{\partial y}\right) = \frac{1}{2}\left(\frac{\partial v_2}{\partial x}\right)$ are the components of infinitesimal rotation tensor in half space.
Therefore Eq. (17) can be transformed as

$$\mu_T\frac{\partial v_3}{\partial x_2} + (\mu_L - \mu_T)(a_1^2\frac{\partial^2 v_3}{\partial x^2} + a_1 a_3\frac{\partial^2 v_3}{\partial x\partial z}) + \mu_T\frac{\partial v_3}{\partial z_2} + (\mu_L - \mu_T)(a_1 a_3\frac{\partial^2 v_3}{\partial z\partial x} + a_3^2\frac{\partial^2 v_3}{\partial x\partial z^2} - \frac{P_2}{4}\frac{\partial^2 v_3}{\partial x^2} = \rho_3\frac{\partial^2 v_3}{\partial t^2} \tag{18}$$

which becomes

$$P\frac{\partial^2 v_3}{\partial z^2} + (Q + \xi_1)\frac{\partial^2 v_3}{\partial x^2} + R\frac{\partial^2 v_3}{\partial x\partial z} = \frac{1}{c_2^2}\frac{\partial^2 v_3}{\partial t^2} \tag{19}$$

where $P = 1 + \left(\frac{\mu_L}{\mu_T} - 1\right) a_3^2$, $Q = 1 + \left(\frac{\mu_L}{\mu_T} - 1\right) a_1^2$, $R = 2a_1 a_3 \left(\frac{\mu_L}{\mu_T} - 1\right)$, $\xi_1 = \frac{-P_2}{4\mu_T}$, $c_2^2 = \frac{\mu_T}{\rho_3}$
Let the solution of Eq. (19) is taken as

$$v_3(x, z, t) = V_3(z) e^{it(x-ct)} \tag{20}$$

where the constants k and c identify as the wave number and phase velocity respectively.
Transforming the PDE of Eq. (19) into second order ODE, it becomes

$$\frac{d^2V_3}{dz^2} + \left(\frac{ikR}{P}\right)\frac{dV_3}{dz} - \frac{1}{P}\left((Q + \xi_1)k^2 - \frac{c^2k^2}{c_2^2}\right)V_3(z) = 0 \tag{21}$$

Therefore, the solution of Eq. (21) looks like below mentioned, for the fiber-reinforced half-space the displacement component as

$$v_3(z) = B_1 e^{-P'z} e^{ik(x-ct)}$$

where $P' = \frac{ikR}{2P} + k\sqrt{\left(\frac{Q+\xi_1}{P}\right) - \frac{R^2}{4P^2} - \frac{c^2}{c_2^2 P}}$

2.5 Boundary Conditions and Finding Dispersion Equation

At the interface between the arid sandy upper region and the piezoelectric layer, as well as at the junction between the piezoelectric layer and the fibre-reinforced medium, it is essential for the mechanical displacements $v_i (i = 1,2,3)$ and shear stress components to satisfy continuity conditions.

1. (a) $v_1 = v_2$ at $z = -H$
(b) $\tau_{yz}^1 = \sigma_{yz}^2$ at $z = -H$
2.(a) $v_2 = v_3$ at $z = 0$
(b) $\sigma_{yz}^2 = \tau_{yz}^3$ at $z = 0$
3. at $z = -H$,

we have taken into account two scenarios since piezoelectric material is present in the model

For electrically open case: Since there is no free charge at the surface so normal component electrical displacement turns into zero, i.e.,

$$D_z(x, -H, t) = 0 \tag{22}$$

and for electrically shorted case: As it is connected to ground so electric potential difference is instantly neutralized, i.e.,

$$\varphi(x, -H, t) = 0 \tag{23}$$

with the help of the above boundary conditions, we have,

$$A_1 . e^{-s_1 H} = C_1 cos(kb_1 H) - C_2 sin(kb_1 H) \tag{24}$$

$$C_1(c_{44} kb_1 sin(kb_1 h) + \frac{e_{15}^2}{\varepsilon_{11}} kb_1 sin(kb_1 h)) + C_2(c_{44} kb_1 cos(kb_1 h) + \frac{e_{15}^2}{\varepsilon_{11}} kb_1 cos(kb_1 h)) + C_3 e_{15} k e^{-kH} - C_4 e_{15} k e^{kH} - \frac{\mu_1}{\eta_1} A_1 s_1 e^{-s_1 H} = 0 \tag{25}$$

$$C_1 = B_1 \tag{26}$$

$$C_2 c_{44} kb_1 + \frac{e_{15}^2}{\varepsilon_{11}} C_2 kb_1 + C_3 e_{15} k - C_4 e_{15} k + \mu_T B_1 P_2 - (\mu_L - \mu_T)(b_1 b_3 ikB_1 - b_3^2 B_1 P_2) = 0 \tag{27}$$

$$\frac{e_{15}}{\varepsilon_{11}} C_1 + C_3 + C_4 = 0 \tag{28}$$

$$C_3 k e^{-kH} - C_4 k e^{kH} = 0 \tag{29}$$

$$C_1 \frac{e_{15}}{\varepsilon_{11}} cos(kb_1 H) - C_2 \frac{e_{15}}{\varepsilon_{11}} sin(kb_1 H) + C_3 e^{-kH} + C_4 e^{kH} = 0 \tag{30}$$

Eliminating all arbitrary constants $A_1, C_1, C_2, C_3, C_4, B_1$ from the above six Equations, ultimately, we have found out the dispersion relation of the SH- wave for the structure investigated in this problem.

2.6 Relation of Dispersion Obtained for Electrically Open Case

By solving Eq. (24) to Eq. (29) from $|a_{ij}| = 0$, we have non-trivial Equations that ultimately gives the dispersion relation for the electrically open case.

2.7 Relation of Dispersion Obtained for Electrically Shorted Case

Solving Eq. (24) to Eq. (28) and Eq. (30) from $|b_{ij}| = 0$, we obtained the dispersion relation for the electrically shorted case.

2.8 Some Cases

Case I

If $\eta = 1$ i.e., the upper medium converts into an elastic one, then the dispersion relation obtained in both the open and shorted cases by solving Eqs. (24) to (29) and Eqs. (24) to (28) and (30), we solved two determinants $|c_{ij}| = 0$ and $|d_{ij}| = 0$ both for electrically open cases and electrically short cases. All c_{ij} and d_{ij} are entries of sixth-order square matrix mentioned in Appendices A and B respectively.

Case II

If we ignore stresses of both the layers by $P_1 \longrightarrow 0$ and $P_2 \longrightarrow 0$, then the dispersion relations are obtained for both electrically open and short cases by solving $|e_{ij}| = 0$ and$|f_{ij}| = 0$. All e_{ij} and $f_{ij}$are entries of sixth-order square matrix mentioned in Appendices C and D respectively.

Case III

If the reinforcement is neglected, i.e., $b_1 = 1, b_2 = b_3 = 0$ then we get the Equations for both electrically open case and short cases by solving $|g_{ij}| = 0$ and$|h_{ij}| = 0$. All g_{ij} and h_{ij} are entries of the sixth-order square matrix mentioned in Appendices E and F respectively.

Case IV

If the piezoelectric coefficient is zero, i.e., $e_{15} \longrightarrow 0$ and$c_{44} *= c_{44}$, then for both electrically open and short case. This equation represents a precisely defined SH- equation for a layer that is both isotropic and homogeneous, positioned atop a substrate that shares the same isotropic and homogeneous characteristics.

3. Results and Discussion

In order to perform the outcome of dry sandy parameter, depth, stress of piezoelectric layer and stress of reinforced layer on the propagation of SH-wave in a three-layer structure; A piezoelectric layer, under initial stress, is positioned between a dry sandy half-space and a fibre-reinforced elastic half-space, both of which are also experiencing initial stress; the details outlined below have been taken into consideration.

(a) Dry sandy half-space [cf. Gubbins [40]

$\mu_1 = 7.54 \times 10^{10}\ N/m^2$; $\rho_1 = 3293\ kg/m^3$

(b) Piezoelectric Material (PZT 4) [Nie et al.,[41]

$c_{44} = 25.6 \times 10^9 N/m^2$,

$e_{15} = 12.7 C/m^2$,

$\varepsilon_{11} = 6.45 \times 10^{-9} C^2/Nm^2$,

$\rho_2 = 7500 kg/m^3$

(c) Fibre-reinforced elastic half space under initial stress [Markham [42]

$\mu_L = 7.07 \times 10^{10} N/m^2$,

$\mu_T = 3.50 \times 10^{10} N/m^2$,

$\rho_3 = 1600 kg/m^3$

Using the non-dimensional phase velocity of the dry sandy layer vertically and the non-dimensional wavenumber horizontally, we've constructed graphs from the dispersion Eqs. (31) and (32), taking into account various values of the multiple non-homogeneous parameters previously outlined. The results imposed by different parameters for the electrically open case are presented in Figures 2-4 and for the electrically shorted case in Figure 5 using the data mentioned above.

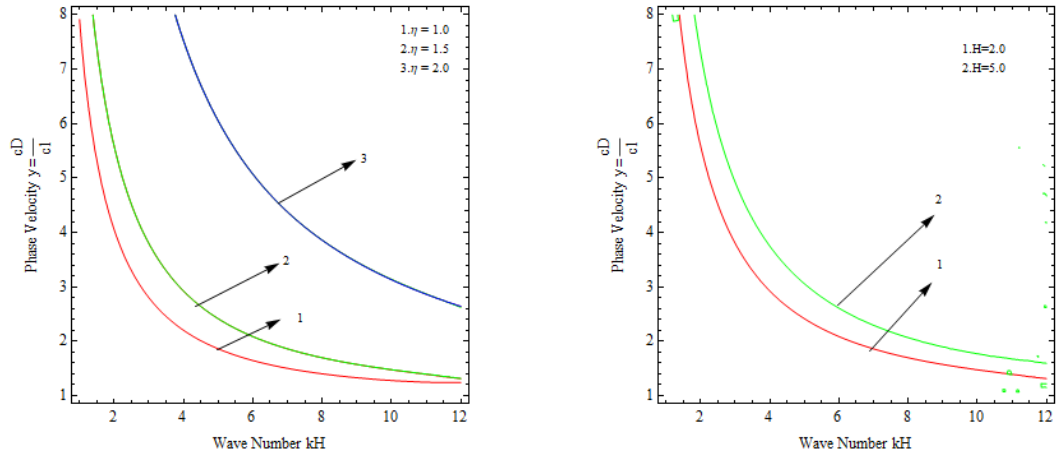

(a) Dry sandy parameter (b) depth of piezo-electric layer

Figure 2. Variation of phase velocity versus wave number for different values of dry sandy parameter and depth of piezo-electric layer for the electrically open case

3.1 Electrically Open Case

Figure 2 shows the effect of the sandy parameter in a dry sandy half-space on the phase velocity of the SH-wave for an electrically open piezoelectric layer. In this figure, the values of η_1 are taken as1.0,1.5,2.0. It shows that the phase velocity decreases as the wavenumber increases. It is clear that dispersion occurs and that the graph is non-linear, indicating that the medium treats wavelengths differently. At high phase velocities and wave numbers, the medium becomes non-dispersive as the curve approaches a flat line. It is clear from the study that long waves penetrate deeper, whereas short waves are confined near the surface. Figure 2(a) demonstrates that wave propagation in the system is inherently dispersive, as the phase velocity decreases with increasing wavenumber, indicating that shorter wavelengths travel more slowly than longer ones. Under electrically open conditions, the piezoelectric layer plays an active role in wave dynamics via electromechanical coupling, thereby significantly enhancing the medium's stiffness. With an increase in the depth of the piezoelectric layer, a larger section of the material engages in this coupling, resulting in a uniform increase in phase velocity for all wave numbers. The effect is especially noticeable for long waves, as these waves interact with the full depth of the layer. However, for short waves (large k_H), the influence of depth diminishes, leading to the convergence of the curves. Overall, Figure 2(a) illustrates that a thicker piezoelectric layer increases wave speed but does not eliminate dispersion, suggesting that both structural geometry and electrical boundary conditions significantly influence wave propagation characteristics in such materials. In Figure 2(b), the values of H were taken as 2.0, 2.5 and 3.0, respectively. It shows that as H increases, phase velocity increases with wavenumber. Figure 3 deliberates the effect of the variation of initial stress in Piezoelectric layer on Phase velocity. The Piezoelectric layer act as a dispersive medium where the value of P_1 increases, material becomes stiffer and so wave speed increases. So, phase velocity increases as initial stress increases. But in respect of wave number phase velocity decreases as wave number increases.

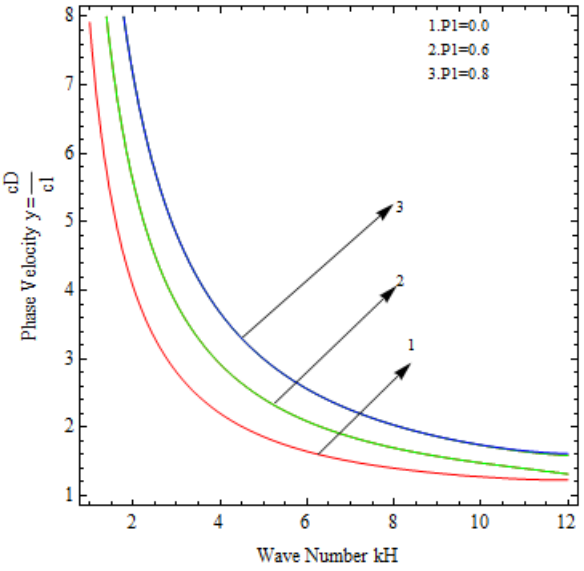

Figure 3. Variation of phase velocity vs. wave number for different values of initial stress of PZT layer for electrically open case

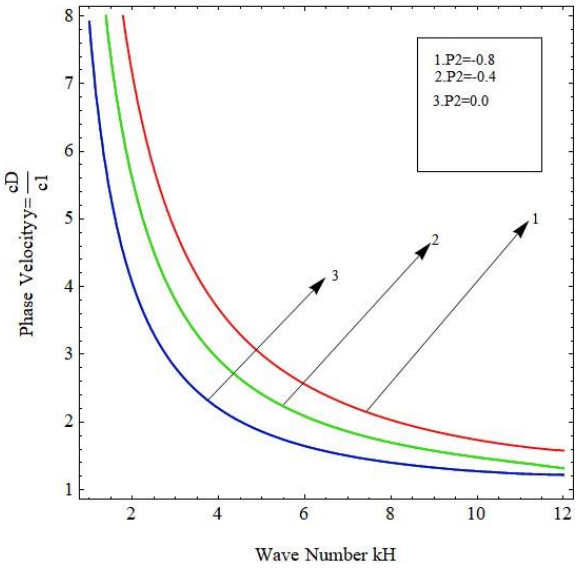

Figure 4. Variation of phase velocity vs. wave number for different values of initial stress of fibre reinforced half space for electrically shorted case

3.2 Electrically Shorted Case

Figure 4 is designed in the context of electrically shorted case. This graph expresses the relation of phase velocity vs. wave number. It deliberates that the phase velocity decreases with the increase of wave number gives a dispersive nature of the fibre reinforced medium. Here the effect of initial stress is important. For the different values of P_2 i.e., -0.8, -0.4, 0.0 we see that increasing comprehensive initial stress upgrades effective stiffness of that medium. This behavior shows how electrically shorted boundary conditions, which keep the electric potential at zero, affect the electromechanical coupling and, in turn, change how SH type waves move through the fibre-reinforced material. Thus, the interplay between electrical boundary conditions, reinforcement anisotropy and pre-stress opens a much greater space for engineering controllable systems and band gaps. The smooth interfaces effectively confine wave energy and prior sensitivity to these parameters. Collectively, the results demonstrate that tri-layered can be transformed into a frequency-selective filter, a stress-transducing sensor or a tunable seismic barrier which can lead to next-generation smart composites.

4. Conclusions

The present work has established a rigorous analytical framework consisting of a dry sandy half-space, a piezoelectric inter-layer, and a fibre-reinforced elastic substrate, all clamped under smooth-contact conditions. The principal findings and their technological implications are as follows:

i) The closed-form dispersion relation reveals that the phase velocity is a strongly non-linear function of the wavenumber, with the sandiness parameter, piezoelectric layer thickness, initial stresses, and electrical boundary conditions each serving as an independent lever to regulate the dispersive nature of the waves. Loosely packedness reduced the overall wave speed, while thicker and pre-stressed piezoelectric layers elevate it, confirming that the composite can be tailored for specific wave-filtering functions.
ii) The piezoelectric intermediate layer introduces an electromechanical coupling which reveals in event of electrically shortedness, the coupling effect is partially suppressed. This duality, combined with the directional anisotropy of the fiber-reinforced substrate generates distinct and controllable band gaps at high wavenumbers, establishing the structure as a robust platform for frequency-selective surface acoustic wave devices.
iii) Smooth contact at both the interface confines wave energy efficiently, which enhances the sensitivity of the dispersion curves to its material properties and geometric parameters. This confinement is especially helpful for sensor applications.
iv) The proposed model correlates the classical geomechanics and modern smart materials, offering large applications: (i) for designing smart barriers that exploit electro-mechanical tuning and absorption of destructive SH-wave energy; (ii) to act as interpretive tool for converting shear-wave splitting in arid or desert regions underlain by reinforced strata, thus improving subsurface imaging; and (iii) for developing SAW sensors employed in structural health monitoring, where the minute dispersion shifts serve as markers of stress, delamination or material degradation.

By furnishing a complete analytical solution and a thorough parametric analysis, this study may provide a platform for future experiments paving the way for the rational design of modern wave-manipulation devices.

Acknowledgements

We would like to thank and acknowledge VIT Bhopal University, Kothrikalan, Sehore, Madhya Pradesh, India for utilising the facilities and laboratories for this project.

Funding

This research did not receive any specific grant from funding agencies in the public, commercial, or not-for-profit sectors.

Declaration of Competing Interest

The author declares no conflicts of interest.

CRediT Authorship Contribution Statement

Suparna Roychowdhury: Conceptualization; Methodology; Writing – original draft
Abhijit Pramanik and Ayan Chatterjee: Conceptualization; Formal analysis
Mostaid Ahmed: Methodology; Writing – review and editing

Availability of Data and Materials

Data sharing is not applicable to this article as no new data were created or analysed in this study.

Ethics Declarations

This study did not involve human participants or animals. Ethical approval was therefore not required.

Generative Artificial Intelligence Declarations

The authors claim that artificially intelligent-assisted technologies, such as generative AI, were not used to generate content, ideas, or theories. We have just utilised AI to enhance readability and refine the language. This was used with extreme human control and oversight. The authors take full responsibility for reviewing and approving the content.

References

[1] J. Achenbach, *Wave propagation in elastic solids*, Elsevier, 2012.

[2] X.P. Li, "Attenuation dispersion of Love waves in a two-layered half space," *Wave motion*, vol. 22, no. 4, pp. 349-370, 1995.

[3] W. H. Weiskopf, "Stresses in soils under a foundation," *Journal of the Franklin Institute*, vol. 239, no. 6, pp. 445-465, 1945.

[4] M. K. Paul, "Propagation of love waves in a dry sandy layer lying between two semi-infinite elastic media," *Acta Geophys Pol*, vol. 13, no. 1, pp. 1-7, 1965.

[5] L. M. Slavin, and B. Wolf, "Scattering of Love waves in a surface layer with an irregular boundary for the case of a rigid underlying half-space," *Bulletin of the Seismological Society of America*, vol. 60, no. 3, pp. 859-877, 1970.

[6] B. Wolf, "Propagation of Love waves in layers with irregular boundaries," *Pure and Applied Geophysics*, vol. 78, no. 1, pp. 48-57, 1970.

[7] A. Chattopadhyay, and A. K. Pal, "SH waves in anisotropic layer with irregular boundary," *Bulletin de l'Académie Polonaise des Sciences. Série des Sciences Techniques*, vol. 30, no. 5-6, pp. 51-59, 1982.

[8] A. Chattopadhyay, "Propagation of SH waves in a viscoelastic medium due to irregularity in the crustal layer," *Bulletin of Calcutta Mathematical Society*, vol. 70, pp. 303-316, 1978.

[9] S. Dey, A. K. Gupta, and S. Gupta, "Effect of gravity and initial stress on torsional surface waves in dry sandy medium," *Journal of Engineering Mechanics*, vol. 128, no. 10, pp. 1115-1118, 2002.

[10] S. S. Singh, "Love wave at a layer medium bounded by irregular boundary surfaces," *Journal of Vibration and Control*, vol. 17, no. 5, pp. 789-795, 2011.

[11] J. Pal, and A. P. Ghorai, "Propagation of Love wave in sandy layer under initial stress above anisotropic porous half-space under gravity," *Transport in Porous Media*, vol. 109, no. 2, pp. 297-316, 2015.

[12] D. K. Pandit, and S. Kundu, "Propagation of Love wave in viscoelastic sandy medium lying over pre-stressed orthotropic half-space," *Procedia Engineering*, vol. 173, pp. 996-1002, 2017.

[13] S. Deep, and V. Sharma, "Love type waves in a dry sandy layer lying over an isotropic elastic half-space with imperfect interface," *Journal of Physics: Conference Series*, vol. 1531, no. 1, p. 012069, 2020.

[14] J. Liu, and S. He, "Properties of Love waves in layered piezoelectric structures," *International Journal of Solids and Structures*, vol. 47, no. 2, pp. 169-174, 2010.

[15] X. Han, and G. R. Liu, "Elastic waves in a functionally graded piezoelectric cylinder," *Smart Materials and Structures*, vol. 126, p. 962, 2003.

[16] J. Du, K. Xian, J. Wang, and Y. K. Yong, "Propagation of Love waves in prestressed piezoelectric layered structures loaded with viscous liquid," *Acta Mechanica Solida Sinica*, vol. 21, no. 6, pp. 542-548, 2008.

[17] M. Eskandari, and H. M. Shodja, "Love waves propagation in functionally graded piezoelectric materials with quadratic variation," *Journal of Sound and Vibration*, vol. 313, no. 1-2, pp. 195-204, 2008.

[18] B. Singh, and S. J. Singh, "Reflection of plane waves at the free surface of a fiber-reinforced elastic half-space," *Sadhana*, vol. 29, no. 3, pp. 249-257, 2004.

[19] S. Behdad, and M. Arefi, "A mixed two-phase stress/strain driven elasticity: In applications on static bending, vibration analysis and wave propagation," *European Journal of Mechanics-A/Solids*, vol. 94, p. 104558, 2022.

[20] S. Behdad, and M. Arefi, "On the dynamics of nanoscale structures upon a novel mixture model of elasticity: buckling analysis, vibration analysis, and wave propagation," *Waves in Random and Complex Media*, vol. 36, no. 3, pp. 4391-4422, 2026.

[21] A. J. Belfield, T. G. Rogers, and A. J. M. Spencer, "Stress in elastic plates reinforced by fibers lying in concentric circles," *Journal of the Mechanics and Physics of Solids*, vol. 31, no. 1, pp. 25-54, 1983.

[22] A. Das, A. K. Singh, P. P. Patel, K. C. Mistri, and A. Chattopadhyay, "Reflection and refraction of plane waves at the loosely bonded common interface of piezoelectric fiber-reinforced and fiber-reinforced composite media," *Ultrasonics*, vol. 94, pp.131-144, 2019.

[23] M. L. Dehsaraji, M. Arefi, and A. Loghman, "Size dependent free vibration analysis of functionally graded piezoelectric micro/nano shell based on modified couple stress theory with considering thickness stretching effect," *Defence Technology*, vol. 17, no. 1, pp. 119-134, 2021.

[24] H. Ezzin, M. Mkaoir, M. Arefi, Z. Qian, and R. Das, "Analysis of guided wave propagation in functionally graded magneto-electro elastic composite," *Waves in Random and Complex Media*, vol. 34, no. 4, pp. 2858-2876 2024.

[25] S. Rakshit, K. C. Mistri, A. Das, and A. Lakshman, "Effect of interfacial imperfections on SH-wave propagation in a porous piezoelectric composite," *Mechanics of Advanced Materials and Structures*, vol. 29, no. 25, pp. 4008-4018, 2022.

[26] A. K. Singh, K. C. Mistri, and A. Das, "Propagation of love-type wave in a corrugated fiber-reinforced layer," *Journal of Mechanics*, vol. 32, no. 6, pp. 693-708, 2016.

[27] A. K. Singh, A. Das, K. C. Mistri, A. Chattopadhyay, "Green's function approach to study the propagation of SH-wave in piezoelectric layer influenced by a point source," *Mathematical Methods in the Applied Sciences*, vol. 40, no. 13, pp. 4771-4784, 2017.

[28] S. Roychowdhury, A. Pramanik, and M. Ahmed, "Analysis of electrically shorted and open cases on love waves propagating in piezoelectric layer embedded over a fiber-reinforced substrate," *Mechanics of Advanced Composite Structures*, vol. 12, no. 1, pp. 1-2, 2024.

[29] S. Gupta, A. Pramanik, M. Ahmed, and A. K. Verma, "Love wave propagation in prestressed piezoelectric layered structure," *International Journal of Applied Mechanics*, vol. 8, no. 4, p.1650045, 2016.
[30] A. K. Singh, A. Das, A. Lakshman, A. and A. Chattopadhyay, "Effect of corrugation and reinforcement on the dispersion of SH-wave propagation in corrugated poroelastic layer lying over a fiber-reinforced half-space," *Acta Geophysica*, vol. 64, pp. 1340-1369, 2016.
[31] S. upta, A. Pramanik, and M. Ahmed, "Impact of pre-stress, inhomogeneity and porosity on the propagation of Love wave," *Acta Geophysica*, vol. 66, pp. 855-866, 2018.
[32] Y. Zhao, P. Li, G. Fan, and C. Shao, "Love wave propagation in a piezoelectric composite structure with an inhomogeneous internal layer," *Materials*, vol. 19, no. 6, p. 1151, 2026.
[33] Sadab, M. and Kundu, S., 2026. Love waves in a piezoelectric microbeam with a loosely bonded interface using Bessel function and finite difference methods. *Journal of the Brazilian Society of Mechanical Sciences and Engineering*, vol. 48, no. 4, p. 297, 2026.
[34] A. K. Rahul, "Love wave propagation across slip interfaces in a viscoelastic orthotropic layer bounded by dry sandy and transversely isotropic media," *Journal of Vibration Engineering & Technologies*, vol. 14, no. 4, p. 199, 2026.
[35] Z. M. Hafizi J. Epaarachchi and K. T. Lau, "Wave propagation scattering due to defects on thin composite plates, *Journal of Mechanical Engineering and Sciences*, vol. 5, no. 1, pp. 602–610, 2013.
[36] J. Fajrin, Y. Zhuge, F. Bullen, and H. Wang, "Flexural behaviour of hybrid sandwich panel with natural fiber composites as the intermediate layer," *Journal of Mechanical Engineering and Sciences*, vol. 10, no. 2, pp. 1968-1983, 2016.
[37] M.S.A. Majid, R. Daud, M. Afendi, N.A.M. Amin, E.M. Cheng, A..G Gibson et al., "Stress-strain response modelling of glass fibre reinforced epoxy composite pipes under multiaxial loadings," *Journal of Mechanical Engineering and Sciences*, vol. 6, no. 1, pp. 916-28, 2014.
[38] B. K. Kar, A. K. Pal, and V. K Kalyani, "Propagation of love waves in an irregular dry sandy layer," *Acta Geophysica Polonica*, vol. 34, no. 2, pp. 157-170, 1986.
[39] A. J. Belfield, T. G. Rogers, and A. J. M. Spencer, "Stress in elastic plates rein forced by fibers lying in concentric circles," *Journal of the Mechanics and Physics of Solids*, vol. 31, no. 1, p. 2554, 1983.
[40] D. Gubbins, *Seismology and plate tectonics*, Cambridge: Cambridge University Press, 1990.
[41] G. Nie, Z. An, and J. Liu, "SH-guided waves in layered piezoelectric/piezomagnetic plates," *Progress in Natural Science*, vol. 19, p. 811–816, 2009.
[42] M. F. Markham, "Measurements of elastic constants of fiber composites by ultrasonics," *Composites*, vol. 1, no. 2, pp. 145-149, 1970.

Appendices
Appendix A

$$c_{11} = e^{-s_1 H}$$
$$c_{12} = -cos(kb_1 H)$$
$$c_{13} = sin(kb_1 H)$$
$$c_{14} = 0$$
$$c_{15} = 0$$
$$c_{16} = 0$$
$$c_{21} = \mu_1 s_1 e^{-s_1 H}$$
$$c_{22} = -c_{44} kb_1 sin(kb_1 H) + \frac{e_{15}^2}{\epsilon_{11}} kb_1 sin(kb_1 H)$$
$$c_{23} = -c_{44} kb_1 cos(kb_1 H) + \frac{e_{15}^2}{\epsilon_{11}} kb_1 cos(kb_1 H)$$
$$c_{24} = e_{15} k e^{-kH}$$
$$c_{25} = e_{15} k e^{kH}$$
$$c_{26} = 0$$
$$c_{31} = 0$$
$$c_{32} = 1$$
$$c_{33} = 0$$
$$c_{34} = 0$$
$$c_{35} = 0$$
$$c_{36} = -1$$

$$c_{41} = 0$$
$$c_{42} = 0$$
$$c_{43} = c_{44}kb_1 + \frac{e_{15}^2}{\epsilon_{11}}kb_1$$
$$c_{44} = e_{15}k$$
$$c_{45} = -e_{15}k$$
$$c_{46} = \mu_T p_2 - (\mu_L - \mu_T)(b_1 b_3 ik - b_3^2 p_2)$$
$$c_{51} = 0$$
$$c_{52} = \frac{e_{15}}{\epsilon_{11}} c_{53} = 0$$
$$c_{54} = 1$$
$$c_{55} = 1$$
$$c_{56} = 0$$
$$c_{61} = 0$$
$$c_{62} = 0$$
$$c_{63} = 0$$
$$c_{64} = ke^{-kH}$$
$$c_{65} = -ke^{-kH}$$
$$c_{66} = 0$$

Appendix B

$$d_{11} = e^{-s_1 H}$$
$$d_{12} = -\cos(kb_1 H)$$
$$d_{13} = \sin(kb_1 H)$$
$$d_{14} = 0$$
$$d_{15} = 0$$
$$d_{16} = 0$$
$$d_{21} = -\mu_1 s_1 e^{-s_1 H}$$
$$d_{22} = c_{44}kb_1 \sin(kb_1 H) + \frac{e_{15}^2}{\epsilon_{11}}kb_1 \sin(kb_1 H)$$
$$d_{23} = c_{44}kb_1 \cos(kb_1 H) + \frac{e_{15}^2}{\epsilon_{11}}kb_1 \cos(kb_1 H)$$
$$d_{24} = e_{15}ke^{-kH}$$
$$d_{25} = e_{15}ke^{kH}$$
$$d_{26} = 0\$$
$$d_{31} = 0$$
$$d_{32} = 1$$
$$d_{33} = 0$$
$$d_{34} = 0$$
$$d_{35} = 0$$
$$d_{36} = -1$$
$$d_{41} = 0$$
$$d_{42} = 0$$
$$d_{43} = c_{44}kb_1 + \frac{e_{15}^2}{\epsilon_{11}}kb_1$$
$$d_{44} = e_{15}k$$
$$d_{45} = -e_{15}k$$
$$d_{46} = \mu_T p_2 - (\mu_L - \mu_T)(b_1 b_3 ik - b_3^2 p_2)$$
$$d_{51} = 0$$
$$d_{52} = \frac{e_{15}}{\epsilon_{11}}$$
$$d_{53} = 0$$
$$d_{54} = 1$$
$$d_{55} = 1$$
$$d_{56} = 0$$

$$d_{61} = 0$$
$$d_{62} = \frac{e_{15}}{\epsilon_{11}} cos(kb_1 H)$$
$$d_{63} = -\frac{e_{15}}{\epsilon_{11}} cos(kb_1 H)$$
$$d_{64} = e^{-kH}$$
$$d_{65} = e^{kH}$$
$$d_{66} = 0$$

Appendix C

$$e_{11} = e^{-s_1 H}$$
$$e_{12} = -cos(kb_1 H)$$
$$e_{13} = sin(kb_1 H)$$
$$e_{14} = 0$$
$$e_{15} = 0$$
$$e_{16} = 0$$
$$e_{21} = -\mu_1 s_1 e^{-s_1 H}$$
$$e_{22} = c_{44} kb_1 \sin(kb_1 H) + \frac{e_{15}^2}{\epsilon_{11}} kb_1 \sin(kb_1 H)$$
$$e_{23} = c_{44} kb_1 \cos(kb_1 H) + \frac{e_{15}^2}{\epsilon_{11}} kb_1 \cos(kb_1 H)$$
$$e_{24} = e_{15} k e^{-kH}$$
$$e_{25} = e_{15} k e^{kH}$$
$$e_{26} = 0$$
$$e_{31} = 0$$
$$e_{32} = 1$$
$$e_{33} = 0$$
$$e_{34} = 0$$
$$e_{35} = 0$$
$$e_{36} = -1$$
$$e_{41} = 0$$
$$e_{42} = 0$$
$$e_{43} = c_{44} kb_1 + \frac{e_{15}^2}{\epsilon_{11}} kb_1$$
$$e_{44} = e_{15} k$$
$$e_{45} = -e_{15} k$$
$$e_{46} = \mu_T p_2 - (\mu_L - \mu_T)(b_1 b_3 ik - b_3^2 p_2)$$
$$e_{51} = 0$$
$$e_{52} = \frac{e_{15}}{\epsilon_{11}}$$
$$e_{53} = 0$$
$$e_{54} = 1$$
$$e_{55} = 1$$
$$e_{56} = 0$$
$$e_{61} = 0$$
$$e_{62} = \frac{e_{15}}{\epsilon_{11}} \cos(kb_1 H)$$
$$e_{63} = -\frac{e_{15}}{\epsilon_{11}} \cos(kb_1 H)$$
$$e_{64} = e^{-kH}$$
$$e_{65} = e^{kH}$$
$$e_{66} = 0$$

where,

$$b_1^2 = \left(\frac{c^2}{c_0^2} - 1\right),$$
$$P^* = \frac{ikR}{2P} + k\sqrt{(\frac{Q}{P}) - \frac{R^2}{4P^2} - \frac{c^2}{c_2^2 P}}$$

Appendix D

$$f_{11} = e^{-s_1 H}$$
$$f_{12} = -\cos(kb_1 H)$$
$$f_{13} = \sin(kb_1 H)$$
$$f_{14} = 0$$
$$f_{15} = 0$$
$$f_{16} = 0$$
$$f_{21} = -\mu_1 s_1 e^{-s_1 H}$$
$$f_{22} = c_{44} kb_1 \sin(kb_1 H) + \frac{e_{15}^2}{\epsilon_{11}} kb_1 \sin(kb_1 H)$$
$$f_{23} = c_{44} kb_1 \cos(kb_1 H) + \frac{e_{15}^2}{\epsilon_{11}} kb_1 \cos(kb_1 H)$$
$$f_{24} = e_{15} k e^{-kH}$$
$$f_{25} = e_{15} k e^{kH}$$
$$f_{26} = 0$$
$$f_{31} = 0$$
$$f_{32} = 1$$
$$f_{33} = 0$$
$$f_{34} = 0$$
$$f_{35} = 0$$
$$f_{36} = -1$$
$$f_{41} = 0$$
$$f_{42} = 0$$
$$f_{43} = c_{44} kb_1 + \frac{e_{15}^2}{\epsilon_{11}} kb_1$$
$$f_{44} = e_{15} k$$
$$f_{45} = -e_{15} k$$
$$f_{46} = \mu_T p_2 - (\mu_L - \mu_T)(b_1 b_3 ik - b_3^2 p_2)$$
$$f_{51} = 0$$
$$f_{52} = \frac{e_{15}}{\epsilon_{11}}$$
$$f_{53} = 0$$
$$f_{54} = 1$$
$$f_{55} = 1$$
$$f_{56} = 0$$
$$f_{61} = 0$$
$$f_{62} = \frac{e_{15}}{\epsilon_{11}} cos(kb_1 H)$$
$$f_{63} = -\frac{e_{15}}{\epsilon_{11}} cos(kb_1 H)$$
$$f_{64} = e^{-kH}$$
$$f_{65} = e^{kH}$$
$$f_{66} = 0$$

where

$$b_1^2 = (\frac{c^2}{c_0^2} - 1),$$

$$P^* = \frac{ikR}{2P} + k\sqrt{(\frac{Q}{P}) - \frac{R^2}{4P^2} - \frac{c^2}{c_2^2 P}}$$

Appendix E

$$g_{11} = e^{-s_1 H}$$
$$g_{12} = -cos(kb_1 H)$$
$$g_{13} = sin(kb_1 H)$$
$$g_{14} = 0$$
$$g_{15} = 0$$
$$g_{16} = 0$$
$$g_{21} = \mu_1 s_1 e^{-s_1 H}$$
$$g_{22} = -c_{44} kb_1 sin(kb_1 H) + \frac{e_{15}^2}{\epsilon_{11}} kb_1 sin(kb_1 H)$$
$$g_{23} = -c_{44} kb_1 cos(kb_1 H) + \frac{e_{15}^2}{\epsilon_{11}} kb_1 cos(kb_1 H)$$
$$g_{24} = e_{15} k e^{-kH}$$
$$g_{25} = e_{15} k e^{kH}$$
$$g_{26} = 0$$
$$g_{31} = 0$$
$$g_{32} = 1$$
$$g_{33} = 0$$
$$g_{34} = 0$$
$$g_{35} = 0$$
$$g_{36} = -1$$
$$g_{41} = 0$$
$$g_{42} = 0$$
$$g_{43} = c_{44} kb_1 + \frac{e_{15}^2}{\epsilon_{11}} kb_1$$
$$g_{44} = e_{15} k$$
$$g_{45} = -e_{15} k$$
$$g_{46} = \mu_T p_2$$
$$g_{51} = 0$$
$$g_{52} = \frac{e_{15}}{\epsilon_{11}}$$
$$g_{53} = 0$$
$$g_{54} = 1$$
$$g_{55} = 1$$
$$g_{56} = 0$$
$$g_{61} = 0$$
$$g_{62} = 0$$
$$g_{63} = 0$$
$$g_{64} = k e^{-kH}$$
$$g_{65} = -k e^{-kH}$$
$$g_{66} = 0$$

Appendix F

$$h_{11} = e^{-s_1 H}$$
$$h_{12} = -cos(kb_1 H)$$
$$h_{13} = sin(kb_1 H)$$
$$h_{14} = 0$$
$$h_{15} = 0$$
$$h_{16} = 0$$
$$h_{21} = -\mu_1 s_1 e^{-s_1 H}$$
$$h_{22} = c_{44} kb_1 sin(kb_1 H) + \frac{e_{15}^2}{\epsilon_{11}} kb_1 sin(kb_1 H)$$
$$h_{23} = c_{44} kb_1 cos(kb_1 H) + \frac{e_{15}^2}{\epsilon_{11}} kb_1 cos(kb_1 H)$$
$$h_{24} = e_{15} k e^{-kH}$$
$$h_{25} = e_{15} k e^{kH}$$
$$h_{26} = 0$$
$$h_{31} = 0$$
$$h_{32} = 1$$
$$h_{33} = 0$$
$$h_{34} = 0$$
$$h_{35} = 0$$
$$h_{36} = -1$$
$$h_{41} = 0$$
$$h_{42} = 0$$
$$h_{43} = c_{44} kb_1 + \frac{e_{15}^2}{\epsilon_{11}} kb_1$$
$$h_{44} = e_{15} k$$
$$h_{45} = -e_{15} k$$
$$h_{46} = \mu_T p_2$$
$$h_{51} = 0$$
$$h_{52} = \frac{e_{15}}{\epsilon_{11}}$$
$$h_{53} = 0$$
$$h_{54} = 1$$
$$h_{55} = 1$$
$$h_{56} = 0$$
$$h_{61} = 0$$
$$h_{62} = 0$$
$$h_{63} = 0$$
$$h_{64} = e^{-kH}$$
$$h_{65} = e^{kH}$$
$$h_{66} = 0$$